

Canadian Committee for the Theory of Machines and Mechanisms



Commission Canadienne pour la Théorie des Machines et des Mécanismes

*2003 CCToMM Symposium on Mechanisms,
Machines, and Mechatronics*

2003 CCToMM M³

*Symposium 2003 sur les mécanismes,
les machines et la mécatronique
de la CCToMM*

May 30, 2003, the Canadian Space Agency, Saint-Hubert (Montréal), Québec,
Canada



Le 30 mai 2003, l'Agence spatiale canadienne, Saint-Hubert (Montréal), Québec,
Canada

FOREWORD

Welcome to the 2003 edition of the Second CCToMM *Symposium on Mechanisms, Machines, and Mechatronics*, or M^3 . We hold M^3 on odd-numbered years. In even-numbered years, we hold our Symposium within the CSME Forum.

We have 29 papers in the symposium proceedings; each of these papers was duly reviewed by two referees. The final version of the papers incorporates the revisions suggested by the referees. The review work was managed by the Review Committee:

Jorge Angeles, McGill University, Symposium Co-Chair and former CCToMM Chair; Roger Boudreau, Université de Moncton, CCToMM Secretary-General; Jozsef Kövecses, Canadian Space Agency; Leila Notash, Queen's University, CCToMM Communications Officer; Jean-Claude Piedboeuf, Canadian Space Agency, Symposium Co-Chair and CCToMM Chair; Ron Podhorodeski, University of Victoria, CCToMM Treasurer. Reviewers were drawn mostly from CCToMM, but, due to the multidisciplinary nature of some papers, we resorted also to external reviewers.

We take the opportunity here to acknowledge the fine review work of all the anonymous reviewers who provided their expertise and their time to make this symposium a technical success. The Canadian Space Agency is to be especially acknowledged for allowing us to use their facilities as the venue of the Symposium, while the Department of Mechanical Engineering and the Centre for Intelligent Machines, McGill University, helped us with the logistics. We also thank Ms. Irène Cartier, McGill University, who acted as an assistant to the Technical Committee and served as a liaison with authors, besides providing her translation expertise and her time to help us with local arrangements.. Scott Nokleby, outgoing CCToMM Student Representative, was instrumental in setting up and updating the Web site of the symposium, while Alexei Morozov, Design Engineer at McGill University's NSERC Design Engineering Chair, provided technical support in the editing of the Proceedings, for which we are deeply thankful.

Jorge Angeles and Jean-Claude Piedboeuf, Symposium Co-Chairs

Montreal and St.-Hubert, May 30, 2003

PRÉFACE

Nous vous souhaitons la bienvenue à l'édition 2003 du Deuxième Symposium sur les mécanismes, les machines et la mécatronique de CCToMM ou M³. Le Symposium M³ se tient à tout les deux ans, en alternance avec le Symposium du Forum CSME.

Les actes du symposium contiennent 29 communications qui furent toutes soumises au processus de revision de deux experts. Les corrections suggérées par les experts ont été incorporées dans la version finale des communications. Le travail de revision a été supervisé par le comité de revision composé des personnes suivantes :

Jorge Angeles, Université McGill, co-organisateur du symposium et ancien président de CCToMM; Roger Boudreau, Université de Moncton, secrétaire général de CCToMM; Jozsef Kövecses, Agence spatiale canadienne; Leila Notash, Queen's University, responsable des communications de CCToMM; Jean-Claude Piedboeuf, Agence spatiale canadienne, co-organisateur du symposium et président de CCToMM; Ron Podhorodeski, Victoria University, trésorier de CCToMM. Les experts provenaient pour la plupart de CCToMM, mais étant donné la multidisciplinarité de certains articles, nous avons eu recours à des experts externes.

Nous profitons de l'occasion pour exprimer notre appréciation pour l'excellent travail de revision anonyme de nos experts, qui ont apporté leur connaissance et leur temps pour faire du symposium un succès. Nous remercions tout spécialement l'Agence spatiale canadienne qui nous permet d'utiliser ses locaux pour la tenue du symposium. Nous reconnaissons également l'apport de services de logistiques du Département de génie mécanique et du Centre de recherches sur les machines intelligentes de l'Université McGill. Nous remercions également Irène Cartier pour son travail d'assistante au comité organisateur, et d'intermédiaire auprès des auteurs. Elle s'est aussi chargée de la traduction de textes. Nous voulons de même souligner le travail de Scott Nokleby, représentant sortant des étudiants à CCToMM, qui s'est occupé de la création et mise à jour du site Web du symposium, tandis que Alexei Morozov, ingénieur de conception à l'emploi de l'Université McGill, dans le cadre de la Chaire CRSNG en génie de la conception, nous a apporté une aide précieuse au plan technique pour la conception et la production des actes du symposium.

Jorge Angeles et Jean-Claude Piedboeuf, co-organisateurs du Symposium

Montréal et St.-Hubert, 30 mai 2003

Table of Contents

Design of Mechanical Elements / Conception d'éléments mécaniques

M3-03-01

A parametric study of planar cam-roller speed reducers
Weimin Zhang, Jorge Angeles, McGill University

M3-03-02

The conceptual design of epicyclic cam trains
Chao Chen, Jorge Angeles, McGill University

M3-03-03

A generalization of the pressure angle
Chao Chen, Jorge Angeles, McGill University

M3-03-04

Synthesis of hypocycloidal gears
N. Nikolov, R. Dolchinkov, V. Galabov, V.N. Latinovic, Concordia University

M3-03-05

Meshing characteristics of hypocycloidal gears
R. Dolchinkov, V. Galabov, N. Nikolov, V.N. Latinovic, Concordia University

Mechanism Design & Visualization / Conception et visualisation de mécanismes

M3-03-06

Design and development of an underactuated finger based on compliant mechanisms
Bruno Massa, Clément Gosselin, Université Laval

M3-03-07

Passive mechanisms with multiple equilibrium configurations
Jing Wang, Clément Gosselin, Université Laval

M3-03-08

CAD data extraction for simulation: An application in Camera Ready View Modelling
Chandan Jordar, Leila Notash, Queen's University

M3-03-09

A model-based visualization technique for mechatronic systems
Jochen Stier, Jens H. Jahnke, University of Victoria

M3-03-10

Optimisation of six-bar Stephenson Dwell linkages using differential evolution
J. Kebrle, D. Koladiya, P.S. Shiakolas, University of Texas at Arlington & Bell Helicopter Textron

*Parallel Robots I / Robots parallèles I***M3-03-11**

Design and prototype of a parallel, wire-actuated robot
Geoff Mroz, Leila Notash, Queen's University

M3-03-12

Kinematic analysis and stiffness mapping of wire-actuated parallel manipulators with rigid branch
Sureyya Sahin, Leila Notash, Queen's University

M3-03-13

Active joint failure analysis of parallel manipulators
Mahir Hassan, Leila Notash, Queen's University

M3-03-14

The effect of joint clearances on the singular configurations of planar parallel manipulators
Marise Gallant, Clément Gosselin, Université Laval

M3-03-15

Type synthesis of input-output decoupled parallel manipulators
Xianwen Kong, Clément Gosselin, Université Laval

*Parallel Robots II / Robots parallèles II***M3-03-16**

Inverse kinematics and dynamics analysis of a three legged parallel mechanism actuated by AGVs
Georgio Rekleitis, Meyer Nahon, Subir Saha, McGill University

M3-03-17

Design manifold of translational parallel manipulators
Xiaoyu Wang, Luc Baron, Guy Cloutier, École Polytechnique de Montreal

M3-03-18

A Graphical solution of the direct kinematic problem of star translational parallel manipulators
Mamdouh Sayd, Luc Baron, Christian Mascle, École Polytechnique de Montreal

M3-03-19

The synthesis of three-degree-of-freedom planar parallel manipulators with revolute joints (3-RRR) for an optimal singularity-free workspace

Marc Arsenault, Roger Boudreau, Université de Moncton

M3-03-20

Robust adaptive neural fuzzy controller based on computed torque control for Manipulators

M. Zeinali, L. Notash, Queen's University

Workspace & Singularities / Espace de travail et singularités

M3-03-21

Frontières d'équilibre de mécanismes à câbles comprenant des liens passifs

Gabriel Côté, Clément Gosselin, Université Laval

M3-03-22

Présence de singularités dans un espace de travail limité

Irina Constantinescu, Clément Gosselin, Université Laval

M3-03-23

Calculs d'espaces de travail à l'aide d'algorithmes de détection de collision: comparaison de deux méthodes

Stéphane Brunet, Luc Baron, École Polytechnique de Montréal

M3-03-24

Identifying the 1-dof-loss velocity-degenerate (singular) configurations of an eight-joint manipulator

Scott Nokleby, Ron P. Podhorodeski, University of Victoria

Geometry Applications & Rolling Robots / Applications géométriques et robots à roues

M3-03-25

Extreme distance to a spatial circle

P. J. Zsombor-Murray, M.J.D. Hayes, M.L. Husty, McGill University

M3-03-26

The modelling of CMM kinematic errors from the geometric guideways errors

T. O. Ekinci, J.R.R. Mayer, École Polytechnique de Montréal

M3-03-27

Influence du comportement dynamique sur la qualité d'une surface fraisée en UGV

Henri Paris, Grégoire Peigné, Daniel Brissaud, Institut National Polytechnique de Grenoble

M3-03-28

The preliminary design of a novel robot for human augmentation
Alessio Salerno, Jorge Angeles, McGill University

M3-03-29

The kinematics of mobile robots with orientable single and dual wheels rolling on a plane
Svetlana Ostrovskaya, Jorge Angeles, McGill University

MESHING CHARACTERISTICS OF HYPOCYCLOIDAL GEARS

N. Nikolov, R. Dolchinkov*, V. Galabov and V.N. Latinovic **

1. Abstract

The paper deals with kinematic characteristics of hypocycloidal gearsets generated by conjugate action of a known pinion with cylindrical teeth. The number of teeth of pinion is for one less than the number of teeth of gear. The line of contact of teeth is analytically formulated and its trends discussed in detail. The effects of the gearset parameters upon the locus of contact points are analytically determined and graphically plotted for the three typical gearsets.

2. Introduction

Cycloidal gearsets are characterized by a large gear ratio when they are designed in a planetary arrangement. The large reductions of input velocity (10 to 50 times) result from the difference of one tooth in numbers of teeth of the pinion and the internal gear. The sizes of the cycloidal gearsets are relatively smaller than those with other shape of tooth profile, including the involute profile, for the same gear ratios and the load ratings. Besides, the loss of power due to friction in these gearsets is reduced to a minimum. These characteristics of cycloidal gears have lead to their increased application in engineering practice [1].

A gearset containing a compound pinion with cylindrical teeth and an internal gear meshing together is shown in Fig.1 Tooth numbers of gear and pinion differ by one.

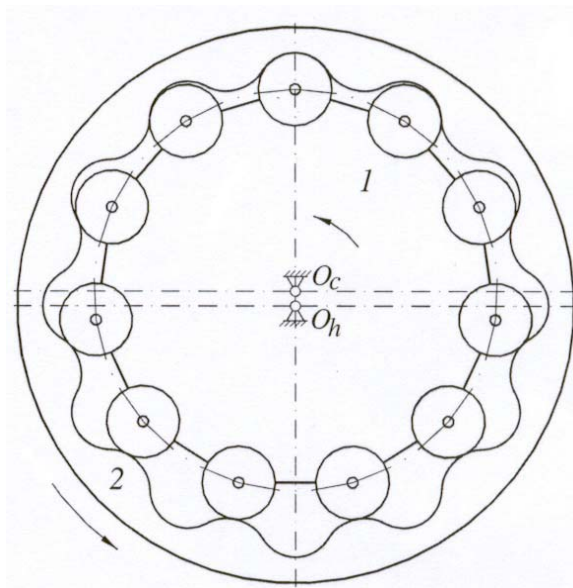


Fig. 1 Gearset of Pinion with Cylindrical Teeth and Epicycloidal Gear with $m=5$ mm, $N_1=11$, $N_2=12$, $x=0.2$ and $r_c^*=1$

In the previous work [3] it has been shown that, besides this gearset, the other two gearsets can be generated, where compound pinion with cylindrical teeth has been replaced by an integral pinion with hypocycloidal external teeth. In this set the tooth profile of the pinion is generated using the conjugate action and external and internal envelope curve of the successive positions of the tooth profile of the hypocycloidal gear in the plain perpendicular to axes of the cenrodes that roll on each other with no slippage.

The objective can be achieved either by use of the theory of envelopes or by utilizing the law of gearing that assumes the instantaneous center of the pinion and gear to be fixed on the line of centers in order to have a constant angular velocities ratio.

In this article the authors aim to investigate the characteristics of meshing of the two hypocycloidal gearsets generated in the above mentioned manner. The locus of contact points is determined for each gearset and the effect of gear parameters upon the line of contact are analytically formulated and discussed. Also the loci of contact points are graphed for the three typical gearsets in Fig. 5.

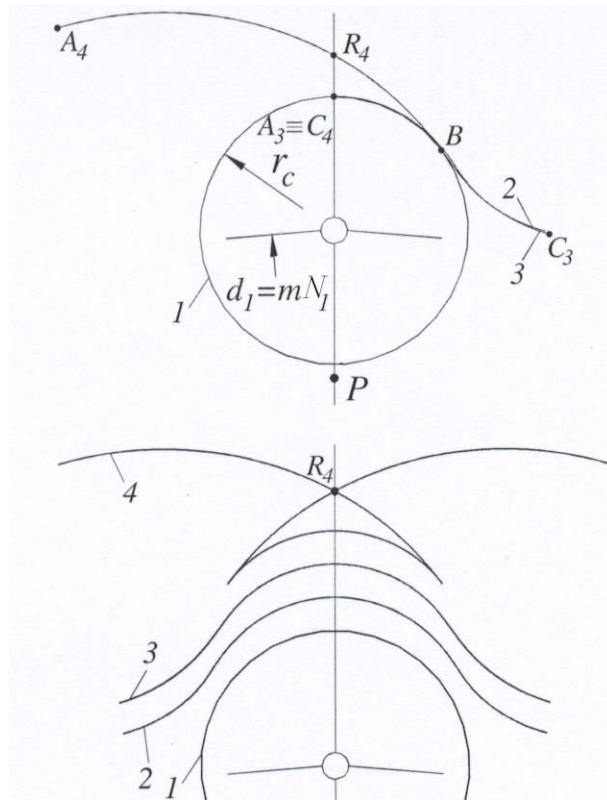


Fig. 2 Conjugate Tooth Profiles of Gearsets 1-2, 3-2 and 4-2 with $N_1=N_3=N_4=11$, $N_2=12$, $x = 0.2$ and $r_c^* = 1$

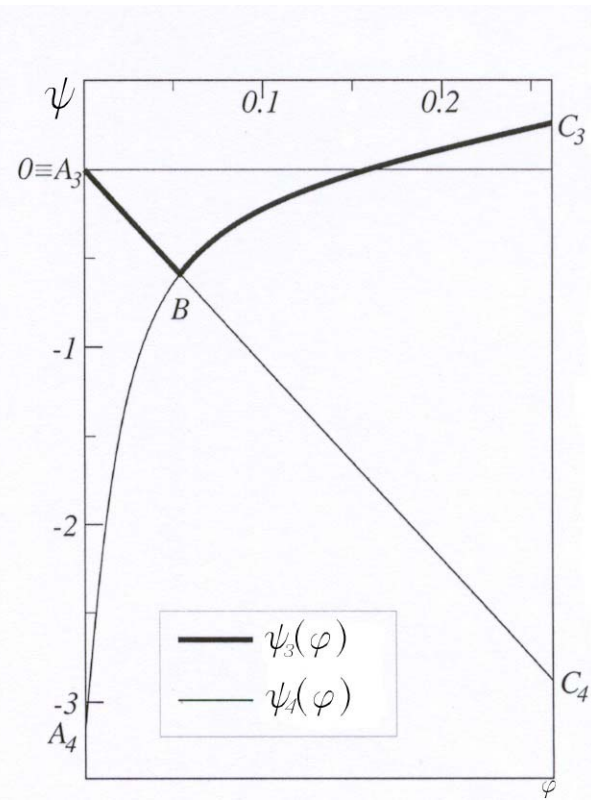


Fig 3 Relation Between Parameters ψ and φ for $N_1=N_3=N_4=11$, $N_2=12$ and $x = 0.2$

3. Determination of Line of Contact

Equations of the tooth profile of hypocycloidal wheel 2 for a typical hypocycloidal gearset are given by:

$$\xi_2 = \frac{m}{2} [(N_2 - 1) \sin \varphi - (1 - x) \sin(N_2 - 1)\varphi + 2r_c^* \frac{(1 - x) \sin(N_2 - 1)\varphi + \sin \varphi}{\sqrt{1 - 2(1 - x) \cos N_2 \varphi + (1 - x)^2}}] \quad (1a)$$

$$\eta_2 = \frac{m}{2} [(N_2 - 1) \cos \varphi - (1 - x) \cos(N_2 - 1)\varphi + 2r_c^* \frac{(1 - x) \cos(N_2 - 1)\varphi + \cos \varphi}{\sqrt{1 - 2(1 - x) \cos N_2 \varphi + (1 - x)^2}}] \quad (1b)$$

where m , N , x and $r_c^* = l$ are module, number of teeth, coefficient of modification (withdrawal) and coefficient of the generating circle radius respectively. The parameter φ varies within interval $[0, \pi/N_2]$. Pinion wheel 1 is of a compound design. It consists of a cylindrical hub and $N_1 = N_2 - 1$ cylindrical teeth of radius $r_c = m r_c^*$ with centres located on a circle with a radius $r = mN_1$. The centre distance is equal to $a_w = 0.5m(1 - x)$.

Two new hypocycloidal gearsets are generated by the pinion with cylindrical teeth, and they consist of hypocycloidal gear 2 with internal teeth, and pinion 3 with external teeth. The hypocycloidal wheel 2 with external teeth and gear 4 with internal teeth as per Fig.2. The tooth profile of the wheels replacing the wheel with cylindrical teeth of the same number of teeth is described in terms of parametric equations:

$$x_{3,4} = \frac{m}{2} [N_1 \sin(\varphi + \frac{\psi_{3,4}}{N_1}) - \lambda \sin(N_1 \varphi - \frac{\psi_{3,4}}{N_1}) - \lambda \sin(\frac{N_2}{N_1} \psi_{3,4}) + 2r_c^* \frac{\lambda \sin(N_1 \varphi - \frac{\psi_{3,4}}{N_1}) - \sin(\varphi + \frac{\psi_{3,4}}{N_1})}{\sqrt{1 - 2\lambda \cos N_2 \varphi + \lambda^2}}] \quad (2a)$$

$$y_{3,4} = \frac{m}{2} [N_1 \cos(\varphi + \frac{\psi_{3,4}}{N_1}) - \lambda \cos(N_1 \varphi - \frac{\psi_{3,4}}{N_1}) - \lambda \cos(\frac{N_2}{N_1} \psi_{3,4}) - 2r_c^* \frac{\lambda \cos(N_1 \varphi - \frac{\psi_{3,4}}{N_1}) - \cos(\varphi - \frac{\psi_{3,4}}{N_1})}{\sqrt{1 - 2\lambda \cos N_2 \varphi + \lambda^2}}] \quad (2b)$$

where $\lambda = 1 - x$ is a factor less than 1, and ψ is the angle of rotation of the hypocycloidal wheel about instantaneous center of velocity P . The angle ψ is defined by equation:

$$\psi_{3,4}(\varphi) = \varphi + \cos^{-1} \frac{-\lambda \sin^2 N_2 \varphi \mp \sqrt{\lambda^2 \sin^4 N_2 \varphi - [\lambda^2 - 2\lambda \cos N_2 \varphi + 1][2\lambda - (1 + \lambda^2) \cos N_2 \varphi] \cos N_2 \varphi}}{\lambda^2 - 2\lambda \cos N_2 \varphi + 1} - \pi \quad (3)$$

The locus of contact points is described by parametric equations:

$$x_k = x_{3,4} \cos(\frac{N_2 \psi_{3,4}}{N_1}) - y_{3,4} \sin(\frac{N_2 \psi_{3,4}}{N_1}) \quad (4a)$$

$$y_k = x_{3,4} \sin(\frac{N_2 \psi_{3,4}}{N_1}) + y_{3,4} \cos(\frac{N_2 \psi_{3,4}}{N_1}) \quad (4b)$$

It is obvious that the tooth-profiles of the wheels 3 and 4, relative to points of contact depend on parameters N_1 , x and r_c^* . In order to define the effect of these parameters, it is necessary to examine the relation (3) between the parameters ψ and φ . It can be concluded:

$$\psi_3(\varphi) = -N_1\varphi, \quad \varphi \in \left[0, \frac{\cos^{-1}(\lambda)}{N_2}\right] \quad (5a)$$

$$\psi_3(\varphi) = \varphi + \cos^{-1} \frac{-\lambda \sin^2 N_2\varphi + (\lambda - \cos N_2\varphi)(\lambda \cos N_2\varphi - 1)}{\lambda^2 - 2\lambda \cos N_2\varphi + 1} - \pi; \quad \varphi \in \left[\frac{\cos^{-1}(\lambda)}{N_2}, \frac{\pi}{N_2}\right] \quad (5b)$$

$$\psi_4(\varphi) = \varphi + \cos^{-1} \frac{-\lambda \sin^2 N_2\varphi + (\lambda - \cos N_2\varphi)(\lambda \cos N_2\varphi - 1)}{\lambda^2 - 2\lambda \cos N_2\varphi + 1} - \pi; \quad \varphi \in \left[0, \frac{\cos^{-1}(\lambda)}{N_2}\right] \quad (5c)$$

$$\psi_4(\varphi) = -N_1\varphi, \quad \varphi \in \left[\frac{\cos^{-1}(\lambda)}{N_2}, \frac{\pi}{N_2}\right] \quad (5d)$$

Obviously within the range $\varphi \in [0, \cos^{-1}(\lambda)/N_2]$ function $\psi_3(\varphi)$ decreases linearly. The same is true for function $\psi_4(\varphi)$ within the range $\varphi \in [\cos^{-1}(\lambda)/N_2, \pi/N_2]$. In order to examine the trend of change of function $\psi_3(\varphi)$ within the range $\varphi \in [\cos^{-1}(\lambda)/N_2, \pi/N_2]$, and of function $\psi_4(\varphi)$ within the range $\varphi \in [0, \cos^{-1}(\lambda)/N_2]$, it is necessary to check the derivative:

$$\frac{d\psi_3(\varphi)}{d\varphi} = \frac{d\psi_4(\varphi)}{d\varphi} = \frac{d\left[\varphi + \cos^{-1} \frac{-\lambda \sin^2 N_2\varphi + (\lambda - \cos N_2\varphi)(\lambda \cos N_2\varphi - 1)}{\lambda^2 - 2\lambda \cos N_2\varphi + 1} - \pi\right]}{d\varphi} \quad (6)$$

After few rearrangements one can obtain the following:

$$\frac{d\psi(\varphi)}{d\varphi} = 1 - \frac{N_2(\lambda^2 - 1)}{\lambda^2 - 2\lambda \cos N_2\varphi + 1}; \quad \varphi \in \left[0, \frac{\pi}{N_2}\right] \quad (7)$$

Since $N_2(\lambda^2 - 1) < 0$, and $\lambda^2 - 2\lambda \cos(N_2\varphi) + 1 > 0$ for $(\lambda \in (0,1))$, one can conclude that $d\psi(\varphi) > 1 > 0$, which means that the function $\psi_3(\varphi)$ within the range $\varphi \in [\cos^{-1}(\lambda)/N_2, \pi/N_2]$ as well as the function $\psi_4(\varphi)$ within the range $\varphi \in [0, \cos^{-1}(\lambda)/N_2]$ are monotonically nondecreasing functions.

The function $\psi_3(\varphi)$ has three extremes as shown in Fig.3. In the range $\varphi \in [0, \cos^{-1}(\lambda)/N_2]$ the function is monotonically decreasing. At $\varphi = 0$ the function has a local maximum equal to zero and at the end of the range at $\varphi_B = \cos(\lambda)/N_2$, it reaches a global minimum equal to $-\cos(\lambda)N_1/N_2$. Within the range $\varphi \in [\cos^{-1}(\lambda)/N_2, \pi/N_2]$ the function is increasing and at the end of the range at value $\varphi = \pi/N_2$ the function reaches a global maximum equal to π/N_2 .

The function $\psi_4(\varphi)$ also has three extremes as shown in Fig 3.. In the range $\varphi \in [0, \cos^{-1}(\lambda)/N_2]$ the function is a monotonically nondecreasing function. At $\varphi = 0$ the function has a global minimum equal to $-\pi$. At $\varphi_B = \cos^{-1}(\lambda)/N_1$ the function reaches a global maximum equal to $-\cos^{-1}(\lambda)N_1/N_2$. Within the range $\varphi \in [\cos^{-1}(\lambda)/N_2, \pi/N_2]$ the function is a monotonically nonincreasing and at $\varphi = \pi/N_2$ it reaches a local minimum equal to $\pi N_1/N_2$.

Fig.4 shows the lines of contact of two hypocycloidal gears with $m = 5$ mm, $N_1 = 11$, $r_c^* = 1$ and $x = 0.2$. Portion of contact line A_3BC_4 corresponding to a linear relation between the parameters ψ and φ , in

both epicycloidal gears is equal to the line of contact of the pinion with cylindrical teeth and the hypocycloidal internal gear. Portion of contact line BC_3 of gerset 3-2 corresponds to line BC_3 of function $\psi_3(\varphi)$ and part BA_4 of gearset 2-4 corresponds to line BA_4 of function $\psi_4(\varphi)$. Gearset 3-2 exhibits two contact points within the range as shown in Fig.4 (a). When $\psi_3(\varphi)$ is changed within the range $\psi_{C_3} = \pi/N_4$ to zero one contact point exists, while within the range from zero to $\psi_B = -\cos^{-1}(\lambda)N_1/N_2$ two contact points occur. Within the range of $\psi_B = -\cos^{-1}(\lambda)N_1/N_2$ to $-\pi N_1/N_2$ only one contact point exists.

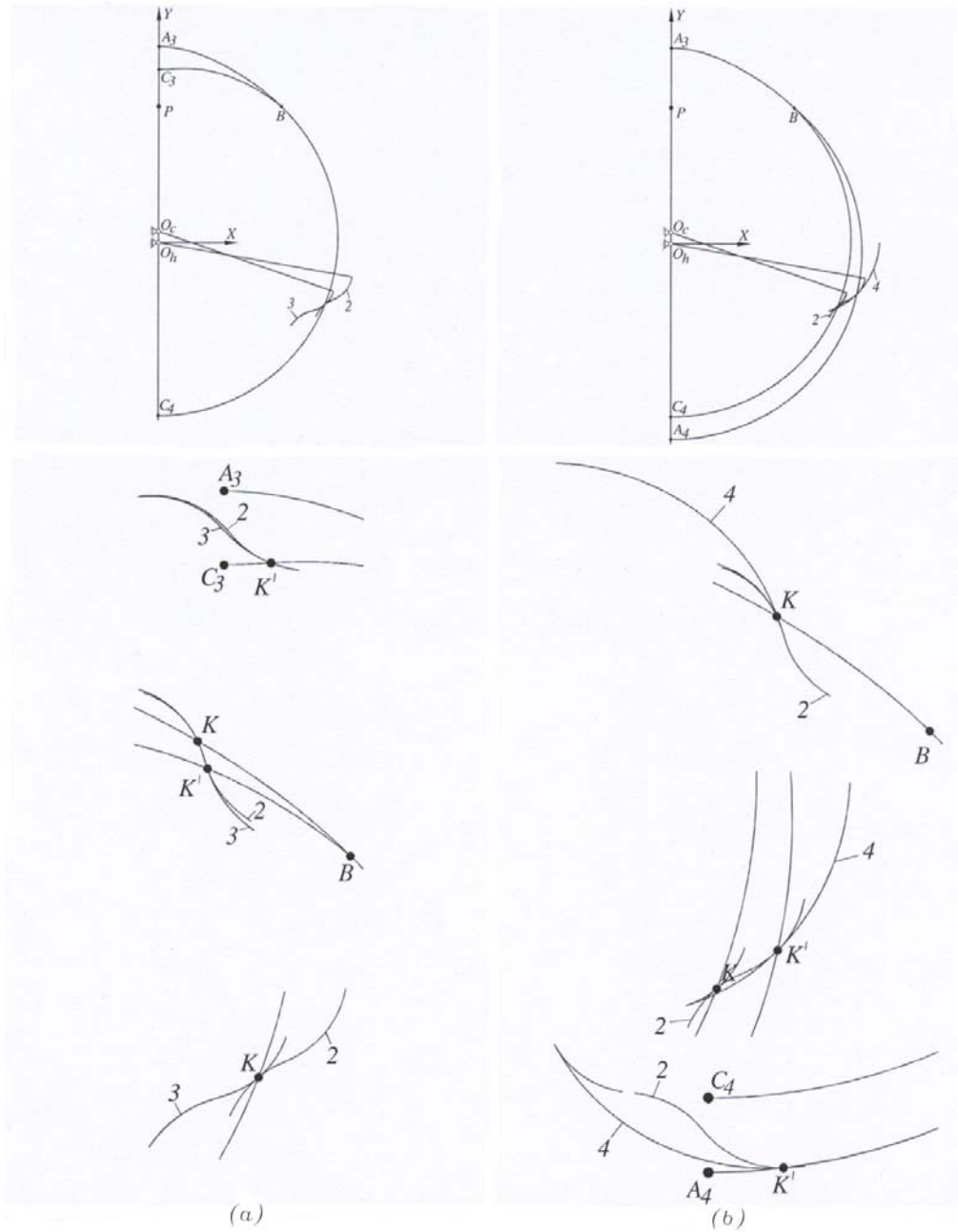


Fig. 4 Lines of Contact of Two Hypocycloidal Gearsets with $m = 5$ mm, $N_1 = 11$, $x = 0.2$ and $r_c^* = 1$

In gearset 2-4 $\psi_4(\varphi)$ also passes through contact ranges with one and two contact points as shown in Fig.4.(b). When $\psi_4(\varphi)$ changes from zero to $\psi_B = -\cos^{-1}(\lambda)N_1/N_2$ one contact point exists. Within the range from $\psi_B = -\cos^{-1}(\lambda)N_1/N_2$ to $-\pi N_1/N_2$ two contact points occur. Within the range from $-\pi N_1/N_2$ to π only one contact point exists. Due to the fact that the profile of gear wheel 4 makes a loop which is undercut so that only part RA_4 remains, there is only one point of contact.

Fig. 5 shows the loci of contact points drawn by a continuous lines for a gearset consisting of a compound pinion with cylindrical teeth and a hypocycloidal pinion and the two hypocycloidal gear generated with $m = 5$ mm, $N_1 = 11$, $x = 0.2$ and $r_c^* = 1$.

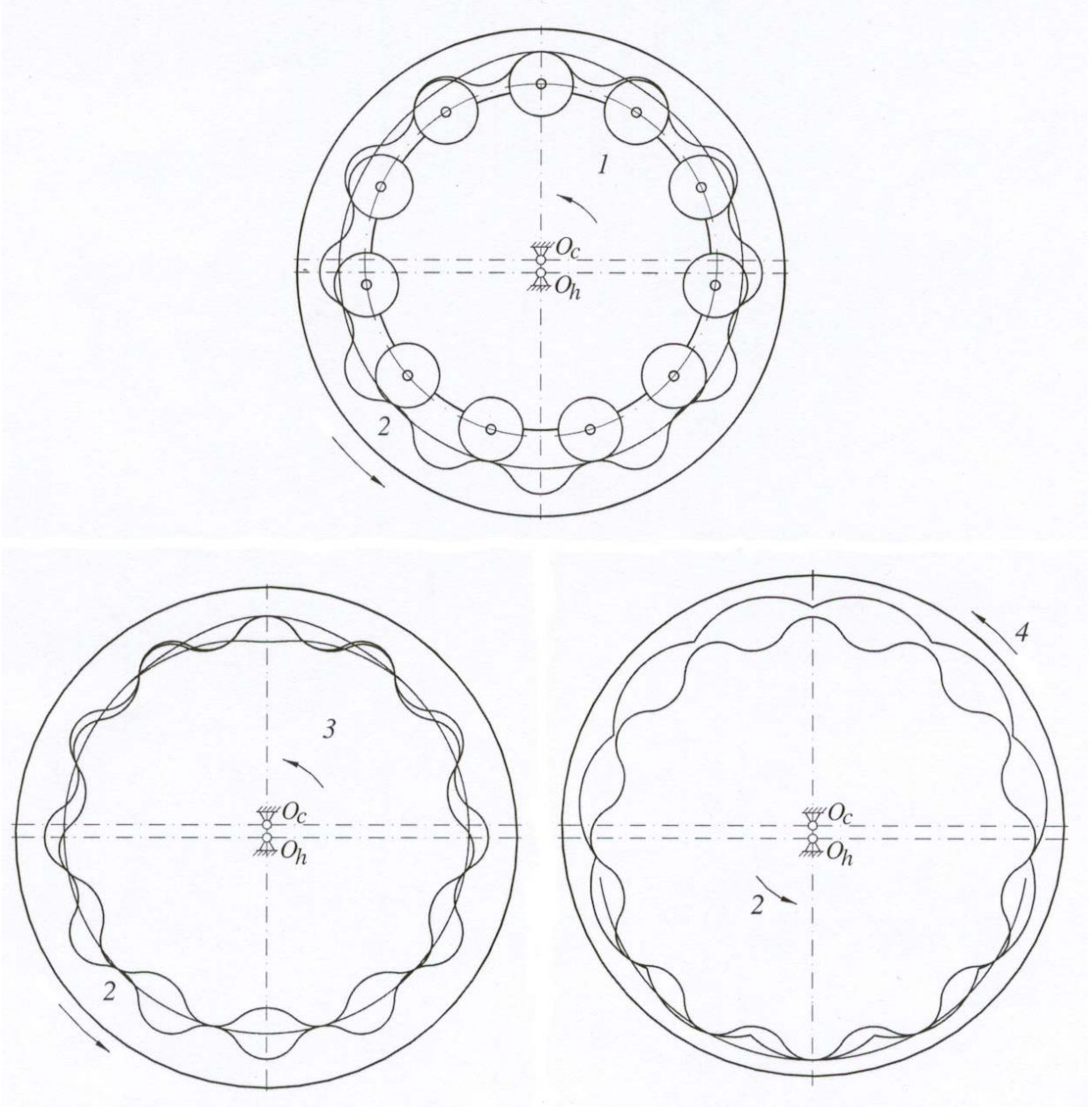


Fig. 5 Lines of Contact for Three Hypocycloidal Gearsets with $m = 5$ mm, $N_1 = 11$, $N_2 = 12$, $x = 0.2$ and $r_c^* = 1$

4. Conclusions

The objective of the study that had been set to generate and analytically formulate parameters of the gearsets based on a pinion with cylindrical tooth profile using the conjugate action and replace the pinion with an integral wheel with hypocycloidal tooth profile has been accomplished. The line of contact has been formulated analytically. The characteristic portions of the line of contact have been critically analyzed and the effect of gearset basic parameters on the line of contact have been established.

As the most important conclusion from the results of this analysis is that generated gearset 3-2 would have an increased load rating because the contact of a convex and a concave surfaces occurs that should yield a lower Hertzian contact stress. In addition a multiple contact points occur along line of contact and an increased load rating could be claimed too. This aspect remains to be investigated by a contact stresses determination. From the property of cycloidal curves the curvature of the surfaces in contact are readily available.

Since the common normal from each contact point must pass through the instantaneous center it is obvious that the pressure angle vary and the transmitted torque is expected to vary. Since there are a half of teeth in contact at any instant it is hoped that the torque will average to a value close to constant.

Gearset 2-4 resulting from the conjugate generating process represents an unusual phenomenon in the theory of the toothed wheels since the number of teeth of wheel 2 is for one larger than the number of teeth of wheel 4, hence designation of the pinion and the gear does not hold anymore. Due to unfavorable pressure angles, as result of undercutting of tooth profile of wheel 4 this gearset is unsuitable for power transmission. Yet, by itself, it is an interesting kinematic phenomenon

References

- [1] Sumitomo, Machinery Corporation of America. Catalog 2001 – “Speed Reducers and Gearmotors” No. 04.301.50.08.
- [2] CYCLO-Gears, Lorenz Braren GmbH, Catalog (in German).
- [3]. Dolchinkov, R., Galabov, Nikolov, N., and Latinovic, V. N., 2003, “Synthesis of Hypocycloidal Gears” CCToMM Symposium on Mechanisms, Machines and Microtronics, May 30, 2003, CSA St. Hubert, Quebec, Canada, to be presented.
- [4] Dolchinkov, R., 2001, Geometry and Forming of Profiled Toothed Wheels in Modified Cyclo-Transmission”, Summary of Ph.D.Dissertation, Burgas, pp.1-46 (in Bulgarian).
- [5] Shigley, J.E. and Uicker, J.J, Jr., 1995, “Theory of Machines and Mechanisms”, McGraw-Hill Book Inc.

Nikolay Nikolov, Ph. D., Assistant Professor, Vitan Galabov, D Sc, Professor , Department of Theory of Mechanisms and Machines, TU Sofia, 8 Kl. Ohridski St., 1000 Sofia, Bulgaria,

*Radostin Dolchinkov, Ph. D., Assistant Professor, Center for Computer Science, Engineering and Natural Sciences, BFU - Bourgas, 8000 Bourgas, Bulgaria.

**V.N. Latinovic , D.Eng., Associate Professor, Department of Mechanical and Industrial Engineering, Concordia University, 1455 de Maisonneuve Blvd. West, Montreal, Quebec, Canada, H3G 1M8.